

Thenar and Hypothenar Muscle Origins on the Transverse Carpal Ligament

¹David B. Jordan, ¹Hui Zhang, ¹Mary N. Henderson, ²C. Kent Kwok, ^{1,2,3}Zong-Ming Li

¹Hand Research Laboratory, Department of Orthopaedic Surgery, University of Arizona, Tucson, Arizona, USA; ²University of Arizona Arthritis Center, Tucson, Arizona, USA; ³Department of Biomedical Engineering, University of Arizona, Tucson, Arizona, USA

Disclosures: Jordan (N), Zhang (N), Henderson (N), Kwok (N), Li (N)

INTRODUCTION: The functionality of the hand is maintained by a complex interplay of muscles, tendons and ligaments. One example is thenar and hypothenar muscles which have origins on the transverse carpal ligament (TCL). [1-2]. These interactive structures play a key role in maintaining the structural stability and functional capability of the thumb and carpal tunnel [3-4]. In order to understand the interaction between the TCL, thenar and hypothenar muscles, with respect to clinical concerns of the hand and wrist, it is necessary to understand the detailed morphological configuration of this interaction. A previous study quantified two-dimensional information regarding the thenar and hypothenar muscle origins at the level of distal carpal tunnel [5], their quantified origin distribution on the TCL surface remains unclear. The purpose of this study was to analyze the three-dimensional volar surface of the TCL, the TCL-thenar interface, and the TCL-hypothenar interface.

METHODS: Ten cadaveric specimens were used for this study (7 female, age 56.6 ± 6.2 years; 3 male, age 57.3 ± 4.7 years). An ultrasound machine with an 18L6 linear array transducer was used to image the carpal tunnel. The ultrasound transducer was mounted into a transducer holder, which was rigidly attached to the end effector of a 6-degrees of freedom robotic arm (Figure 1). Each specimen was placed onto a stabilizing device with the wrist secured in the neutral position, the four fingers secured in extension and the thumb secured in zero degrees of abduction. The robotic arm was moved to position the probe perpendicular to the wrist at the proximal tunnel. A custom LabVIEW program controlled the robot arm to translate the probe distally with a step size of 1 mm for a total scan length of 40 mm. The scanning length was chosen to capture the entire length of the carpal tunnel. At each translational step, an ultrasound image was recorded. To determine the TCL boundary, four bony landmarks, the hook of hamate, ridge of trapezium, tubercle of scaphoid and pisiform, to which the TCL was attached, were identified. In each ultrasound image, the volar surface of the TCL, the TCL-thenar interface, and the TCL-hypothenar interface were manually identified and segmented using a custom MATLAB program (Figure 2A). The collection of two-dimensional points were converted to a three-dimensional point cloud, and then converted into triangular meshes (Figure 2B). The total area of the TCL volar surface, TCL-thenar interface area, TCL-hypothenar interface area were calculated and normalized relative to the TCL volar surface area. For each specimen the total proximal-distal TCL length was calculated. The proximal-distal length of the TCL was normalized relative to the total proximal-distal length, with 0% being at the most proximal tunnel level and 100% being at the most distal tunnel level (Figure 2B). The radial-ulnar length of the TCL-thenar interface, TCL-hypothenar interface, and TCL-alone portion were analyzed at each 10% increment of proximal-distal length, and normalized relative to the total radial-ulnar length of the TCL volar surface. One-way ANOVAs with repeated measures were used to compare the relative areas ($\alpha = 0.05$). Two-way ANOVAs with repeated measures were used to examine the dependence of TCL-muscle interface relative radial-ulnar length on muscle and relative proximal-distal location ($\alpha = 0.05$).

RESULTS: The total surface area of the TCL volar surface was $457.4 \pm 62.2 \text{ mm}^2$ and was comprised of the TCL-thenar interface, TCL-hypothenar interface and TCL-alone surface areas (Figure 3). The surface areas of the TCL-thenar interface, TCL-hypothenar interface and TCL-alone portion were $142.3 \pm 38.0 \text{ mm}^2$ and $32.3 \pm 22.4 \text{ mm}^2$ and $282.72 \pm 40.8 \text{ mm}^2$, respectively. The one-way repeated measures ANOVA showed that the relative TCL-thenar interface area, relative TCL-hypothenar interface area, and relative TCL-alone area were significantly different ($p < 0.001$). The two-way repeated measures ANOVA showed that the relative radial-ulnar length of the interfaces was significantly affected by muscle groups ($p < 0.001$) and by proximal-distal tunnel levels ($p < 0.001$). The relative radial-ulnar length of the TCL-thenar interface was greater than the relative radial-ulnar length of the TCL-hypothenar interface at the 40%, 50%, 60%, 70%, 80%, 90% and 100% proximal-distal tunnel levels (all $p < 0.001$).

DISCUSSION: This study quantified the thenar and hypothenar muscle origins on the TCL. These results were achieved by analyzing the three-dimensionally reconstructed surfaces of the TCL and muscle origins, which were developed from a series of two-dimensional ultrasound images. When compared to the TCL-thenar interface, the TCL-hypothenar interface area and relative radial-ulnar length percentages were less. Due to the larger physiological cross-sectional areas of the thenar muscles [6], the thenar muscles have larger force generation capabilities than the hypothenar muscles, thus greater area and radial-ulnar length percentage of the TCL-thenar interface would be necessary for the anchorage and force generation of the thenar muscles. Clinically, knowledge of muscle origin distribution on the TCL can help to optimize preservation of the muscle-ligament interaction during surgical intervention involving the TCL.

SIGNIFICANCE/CLINICAL RELEVANCE: Quantification of the three-dimensional muscle coverage on the TCL can advance anatomical understanding, inform biomechanical mechanisms for utilizing the muscle-ligament interaction, and minimize potential functional disruption of carpal tunnel release.

REFERENCES: [1] Van Sint Jan et al., Surgical and Radiologic Anatomy, 14, 325-329, 1992. [2] Stecco et al., J Hand Surg Am, 35, 746-753, 2010. [3] Gupta et al., Hand Clin, 28, 1-7, 2012. [4] Pasquella et al., Hand Clin, 28, 19-25, 2012. [5] Alsafar et al., J Wrist Surg, 11, 150-153, 2022. [6] Brand et al., J Hand Surg, 6, 209-219, 1981.

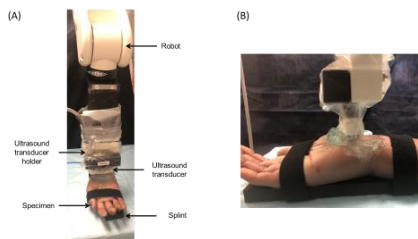


Figure 1. Experimental setup. An ultrasound probe was attached to a robotic arm for proximal to distal ultrasound scanning of the carpal tunnel. (A) Distal view. (B) Ulnar view.

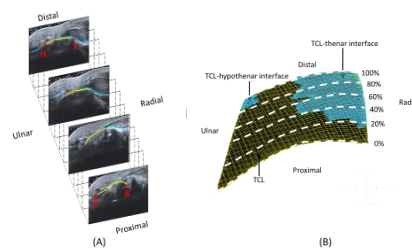


Figure 2. Generation of three-dimensional mesh of the TCL, thenar and hypothenar muscles from segmentation of two-dimensional ultrasound images. (A) The TCL (yellow), thenar and hypothenar muscles (blue) were manually segmented from the ultrasound images. (B) A three-dimensional mesh of the TCL, TCL-thenar interface and TCL-hypothenar interface was generated from the segmentation data.

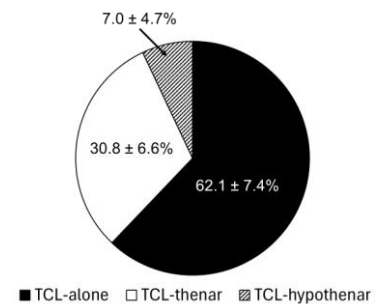


Figure 3. Percentages of the total area of the TCL volar surface occupied by the TCL-thenar interface area, TCL-hypothenar interface area and TCL-alone area.